Proceedings of the Czech–Japanese Seminar in Applied Mathematics 2005
Kuju Training Center, Oita, Japan, September 15-18, 2005
pp. 1–8

NUMERICAL SOLUTION FOR SURFACE DIFFUSION ON GRAPHS

MICHAL BENEŠ[1]

Abstract. The article studies the motion of graphs by the surface Laplacian of the mean curvature by means of the numerical algorithm based on the method of lines with the finite differences in space. The semi-discrete scheme is analysed from the viewpoint of several integral properties and is then used for the computations. We also present the numerical convergence results and investigate the nonlinear dynamics of the problem.

Key words. Surface diffusion, elastic flow, mean curvature, finite differences, Runge-Kutta method.

AMS subject classifications. 35K55, 35K35, 65N06, 65N12, 65N40, 74N20, 74R20

1. Introduction.

This contribution deals with the evolution law

$$V = \Delta_\Gamma(H + F) \text{ on } \Gamma, \tag{1.1}$$

for two-dimensional surfaces Γ embedded in the Euclidean three-dimensional space $\mathbb{R}^3$, which can be represented by graphs. Here, we denoted:

- Γ surface in $\mathbb{R}^3$,
- $\mathbf{n}_\Gamma$ normal vector to Γ,
- V is normal velocity of Γ,
- Δ_Γ is Laplace-Beltrami operator with respect to Γ,
- H is mean curvature of Γ,
- F forcing term.

We study this evolution law within the context of solid state physics and material science. The mentioned law (1.1) is described, e.g. in the results of Mullins [17], [18] as a mechanism of surface formation under the action of chemical potential. Further interesting application is in the microcrack formation as given in [1]. Phenomenology of the problem is studied, e.g. in [8], [6]. Mathematical aspects of the problem are partially discussed in [12], [11], computationally interesting results have been collected in [7], [2], [10].

The purpose of the research is to provide a suitable tool for the study of surfacial phenomena accompanying special surface treatment or behaviour of surfaces under the influence of external forces. The extensive resource of such phenomena can be found in the current research, as indicated by [13], [14].

The general field of application of the developed model can be in:

- body-shape dynamics as a result of surfacial processes,
- surface destruction as a result of external stress and vibration,
- computer data processing.

We also mention a certain diversity in the physical and mathematical terminology, as indicated by [16]. Mathematical understanding of this phenomenon is related to the shape changes due to the redistribution of the matter below the surface, whereas physical investigation considers the surfacial atomic redistribution processes.

[1]Faculty of Nuclear Sciences and Physical Engineering, Czech Technical University in Prague, Trojanova 13, 120 00 Prague, Czech Republic

The parametric form of the evolution law has been studied in [10], the cylindrically symmetric case in [9]. The graph evolution law has been extensivelly studied in [3], to which we refer in the following text. Our approach is similar to the work [19] where the Willmore flow is numerically treated by the method of lines.

2. The evolution for a graph. Our scope is given by the fact that we intend to study the evolution of surfaces as graphs of real functions of two variables. More precisely, we assume that there is a function $\Phi : \mathbb{R}^{1+2} \to \mathbb{R}$ such that

$$\Gamma(t) = \{[x, y] \in \mathbb{R}^3 \mid y = \Phi(t, x), x \in \Omega \subset \mathbb{R}^2\}.$$

For simplicity, we assume that $\Omega = (0, L_1) \times (0, L_2) \subset \mathbb{R}^2$ is an open rectangle, we also denote by $\partial\Omega$ its boundary, by $\mathbf{n}_{\partial\Omega}$ its outer normal and by ∂_n the normal derivative with respect to $\mathbf{n}_{\partial\Omega}$.

Consequently, we express the quantities appearing in (1.1) in terms of this assumption:

$$\begin{aligned} Q(\nabla\Phi) &= \sqrt{1 + |\nabla\Phi|^2}, \\ \tilde{\mathbf{N}} &= [\mathbf{N}, \mathbf{N}_3] = [-\frac{\nabla\Phi}{Q(\nabla\Phi)}, \frac{1}{Q(\nabla\Phi)}], \\ V &= \frac{1}{Q(\nabla\Phi)} \frac{\partial\Phi}{\partial t}, \\ H &= [\nabla, \partial_y] \cdot \tilde{\mathbf{N}} = \nabla \cdot \mathbf{N}, \end{aligned}$$

where $\tilde{\mathbf{N}} = [\mathbf{N}, \mathbf{N}_3]$ is the normal vector to Γ, $\nabla = [\partial_{x_1}, \partial_{x_2}]$ the gradient with respect to $x = [x_1, x_2] \in \Omega$. If $g : \mathbb{R}^2 \to \mathbb{R}$ is a suitable smooth function, $g = g(x)$, we express the Laplace-Beltrami gradient ∇_Γ of g, and the Laplace-Beltrami operator Δ_Γ of g as follows:

$$\begin{aligned} \nabla_\Gamma g &= [\nabla, \partial_y] g - ([\nabla, \partial_y] g \cdot \tilde{\mathbf{N}}) \tilde{\mathbf{N}} = [\nabla g, 0] - ([\nabla g, 0] \cdot \tilde{\mathbf{N}}) \tilde{\mathbf{N}}, \\ &= [\nabla g - (\nabla g \cdot \mathbf{N}) \mathbf{N}, -(\nabla g \cdot \mathbf{N}) \mathbf{N}_3], \\ \Delta_\Gamma g &= (\nabla_\Gamma \cdot \nabla_\Gamma) g. \end{aligned}$$

Consequently, we obtain

$$\begin{aligned} \Delta_\Gamma g &= \sum_{ij=1}^{3} (\delta_{ij} - \mathbf{N}_i \mathbf{N}_j) \, \partial_{ij} g - H \sum_{i=1}^{3} \partial_i g \mathbf{N}_i = \sum_{ij=1}^{2} (\delta_{ij} - \mathbf{N}_i \mathbf{N}_j) \, \partial_{ij} g - H \sum_{i=1}^{2} \partial_i g \mathbf{N}_i \\ &= \Delta g - \mathbf{N}^T g'' \mathbf{N} - H \nabla g \cdot \mathbf{N}, \end{aligned}$$

where ∂_i denotes the partial derivative with respect to the i-th component of x, ∂_{ij} denotes corresponding second partial derivative, g'' denotes the corresponding Hessian matrix.

By substituting the above given quantities into (1.1), we obtain the evolution equations

$$\frac{1}{Q(\nabla\Phi)} \frac{\partial\Phi}{\partial t} = \Delta(H + F) - \frac{(\nabla\Phi)^T (H + F)'' \nabla\Phi}{Q(\nabla\Phi)^2} - H \frac{\nabla(H + F) \cdot \nabla\Phi}{Q(\nabla\Phi)}, \tag{2.1}$$

$$H = -\nabla \cdot \left(\frac{\nabla\Phi}{Q(\nabla\Phi)} \right), \tag{2.2}$$

which are viewed as the fourth-order PDE with respect to Φ. For simplicity, it is endowed by the Dirichlet boundary conditions:

$$\Phi|_{\partial\Omega} = 0, \quad H|_{\partial\Omega} = 0, \tag{2.3}$$

or alternatively, by the Neumann boundary conditions:

$$\left.\frac{\partial\Phi}{\partial n}\right|_{\partial\Omega} = 0, \quad \left.\frac{\partial H}{\partial n}\right|_{\partial\Omega} = 0, \tag{2.4}$$

and by the initial condition

$$\Phi|_{t=0} = \Phi_{ini}. \tag{2.5}$$

The boundary conditions (2.3)/(2.4) can be generalized.

Remark. We shall see later that the boundary conditions (2.4) will be accompanied by the condition

$$\left.\frac{\partial F}{\partial n}\right|_{\partial\Omega} = 0, \tag{2.6}$$

imposed on the forcing term in (1.1).

The evolution equation (2.1) can be rewritten into the divergence form which is more useful from the viewpoint of analysis as well as numerical treatment.

LEMMA 2.1. *The system (2.1) has an algebraically equivalent form*

$$\begin{aligned} \frac{\partial\Phi}{\partial t} &= \nabla\cdot\left(Q(\nabla\Phi)(\nabla(H+F) - (\nabla(H+F)\cdot\mathbf{N})\mathbf{N}\right), \\ H &= -\nabla\cdot\left(\frac{\nabla\Phi}{Q(\nabla\Phi)}\right). \end{aligned} \tag{2.7}$$

Proof. Assuming that the terms in (2.7) are smooth enough we perform the differentiation of (2.7) and obtain

$$\begin{aligned} \frac{\partial\Phi}{\partial t} = {} & Q(\nabla\Phi)\Delta(H+F) + \nabla Q(\nabla\Phi)\cdot(\nabla(H+F) - (\nabla(H+F)\cdot\mathbf{N})\mathbf{N}) \\ & -Q(\nabla\Phi)\mathbf{N}^T(H+F)''\mathbf{N} - Q(\nabla\Phi)(\nabla(H+F)\cdot\mathbf{N})(\nabla\cdot\mathbf{N}) \\ & -Q(\nabla\Phi)(\nabla(H+F)\cdot\mathbf{N}\nabla\mathbf{N}). \end{aligned}$$

Taking into account the fact that

$$\mathbf{N}\nabla\mathbf{N} = \frac{1}{Q(\nabla\Phi)}\left(\nabla Q(\nabla\Phi) - (\mathbf{N}\cdot\nabla Q(\nabla\Phi))\mathbf{N}\right),$$

we obtain the equality

$$\frac{\partial\Phi}{\partial t} = Q(\nabla\Phi)\Delta(H+F) - Q(\nabla\Phi)\mathbf{N}^T(H+F)''\mathbf{N} + Q(\nabla\Phi)H(\nabla(H+F)\cdot\mathbf{N}),$$

which represents the equation (2.1). **q.e.d.**

3. Several mathematical aspects of the evolution law. We denote:

$$(u,v) = \int_\Omega uv\ dx \text{ for } u,v \in \mathrm{L}_2(\Omega).$$

Using standard approach to the weak formulation of an initial-boundary value problem, we multiply the equation (2.7) by a test function Ψ and the equation (2.2) by a test function K ($\Psi, K \in \mathrm{H}_0^1(\Omega)$ for the homogeneous boundary conditions of the type (2.3), $\Psi, K \in \mathrm{H}^1(\Omega)$ for the homogeneous boundary conditions of the type (2.4)), and integrate over Ω. The use of Green's formula yields

$$\begin{aligned}(\frac{\partial\Phi}{\partial t},\Psi) &= \int_{\partial\Omega} \Psi\,(Q(\nabla\Phi)(\nabla(H+F) - (\nabla(H+F)\cdot\mathbf{N})\mathbf{N})\cdot\mathbf{n}_{\partial\Omega}dS \\ &\quad -(Q(\nabla\Phi)(\nabla(H+F)\cdot\nabla\Psi - (\nabla(H+F)\cdot\mathbf{N})(\nabla\Psi\cdot\mathbf{N})),1),\\ (H,K) &= -\int_{\partial\Omega} K(\frac{\nabla\Phi}{Q(\nabla\Phi)}\cdot\mathbf{n}_{\partial\Omega}dS + (\frac{\nabla\Phi}{Q(\nabla\Phi)},\nabla K).\end{aligned}$$

The boundary integrals vanish due to the boundary conditions and we obtain the following definition:

Definition 3.1. *Let $F = F(x)$ be a forcing term, $F \in \mathrm{H}^1(\Omega)$. The weak solution for the problem with homogeneous Dirichlet boundary conditions is a couple $\Phi, H : (0,T) \to \mathrm{H}_0^1(\Omega)$ which satisfies a.e. in $(0,T)$, for each $\Psi, K \in \mathrm{H}_0^1(\Omega)$*

$$\begin{aligned}(\frac{\partial\Phi}{\partial t},\Psi) + (Q(\nabla\Phi)(\nabla(H+F)\cdot\nabla\Psi - (\nabla(H+F)\cdot\mathbf{N})(\nabla\Psi\cdot\mathbf{N})),1) = 0, \quad (3.1)\\ (H,K) - (\frac{\nabla\Phi}{Q(\nabla\Phi)},\nabla K) = 0,\end{aligned}$$

and the initial condition

$$\Phi|_{t=0} = \Phi_{ini}.$$

Weak solution for the problem with homogeneous Neumann boundary conditions is a couple $\Phi, H : (0,T) \to \mathrm{H}^1(\Omega)$ which satisfies the equalities a.e. in $(0,T)$, for each $\Psi, K \in \mathrm{H}^1(\Omega)$.

Naturally, there is a close relationship between the strong and weak formulation of the problem (1.1) as indicated in the following statement:

Lemma 3.2. *Let Φ, H be a solution to the initial-boundary value problem (3.1) which is smooth enough. Then it is the strong solution for (2.1).*

The proof is simple and is mentioned, e.g. in [3].

Regardless of the chosen form of the graph evolution law (1.1), we observe the following features of its solution. Most of them can also be found in [3]. We provide their proof for better understanding of the analysis of our numerical scheme presented later in the text.

Lemma 3.3. *Let Φ, H be a solution to the initial-boundary value problem (2.7) with $F = 0$. Then the following property holds*

$$\frac{d}{dt}\int_\Omega \Phi dx = 0,$$

provided the boundary conditions (2.4) are imposed.

Proof. We integrate the equation (2.7) over Ω and use Green's formula:

$$\frac{d}{dt}\int_\Omega \Phi dx = \int_{\partial\Omega} (Q(\nabla\Phi)(\nabla(H+F) - (\nabla(H+F)\cdot\mathbf{N})\mathbf{N})\cdot\mathbf{n}_{\partial\Omega} dS.$$

The boundary integral vanishes provided $F = 0$ and the pair of homogenous Neumann boundary conditions is applied. **q.e.d.**

LEMMA 3.4. *Let Φ, H be a solution to the initial-boundary value problem (2.7) with $F = 0$. Then the following property holds*

$$\frac{d}{dt}\int_\Omega Q(\nabla\Phi)dx + \int_\Omega \left(|\nabla H|^2 - |\nabla H\cdot\mathbf{N}|^2\right) Q(\nabla\Phi)dx = 0,$$

provided the boundary conditions either (2.3), or (2.4) are imposed.

Proof. The energy equality to prove is obtained by investigating the left-hand side as follows:

$$\frac{d}{dt}\int_\Omega Q(\nabla\Phi)dx = \int_\Omega \frac{\nabla\partial_t\Phi\cdot\nabla\Phi}{Q(\nabla\Phi)}dx = \int_{\partial\Omega}\frac{\partial_t\Phi}{Q(\nabla\Phi)}\frac{\partial\Phi}{\partial n}dS - \int_\Omega \partial_t\Phi\nabla\cdot\frac{\nabla\Phi}{Q(\nabla\Phi)}dx.$$

The boundary integral vanishes due to (2.3)/(2.4). Then, using (2.7)

$$\begin{aligned}
&-\int_\Omega \partial_t\Phi\nabla\cdot\frac{\nabla\Phi}{Q(\nabla\Phi)}dx = \int_\Omega H\nabla\cdot\left(Q(\nabla\Phi)(\nabla(H+F) - (\nabla(H+F)\cdot\mathbf{N})\mathbf{N}\right)dx\\
&= \int_{\partial\Omega} HQ(\nabla\Phi)(\nabla(H+F) - (\nabla(H+F)\cdot\mathbf{N})\mathbf{N}\cdot\mathbf{n}_{\partial\Omega}dS\\
&-\int_\Omega Q(\nabla\Phi)(|\nabla H|^2 - (\nabla H\cdot\mathbf{N})^2)dx,
\end{aligned}$$

where the boundary integral again vanishes due to (2.3)/(2.4) and due to the assumption $F = 0$. **q.e.d.**

4. Discretization. For the purpose of numerical solution of the law (2.7), we derive a numerical scheme based on the method of lines together with the finite-difference discretization of spatial derivatives. We introduce the following notation (g is a suitable, at least continuous function defined on $\bar\Omega$):

$$\begin{aligned}
\mathbf{h} &= (h_1, h_2)\,,\ h_1 = \frac{L_1}{N_1},\ h_2 = \frac{L_2}{N_2},\\
\omega_h &= \{[ih_1, jh_2] \mid i = 1,\dots,N_1-1;\ j = 1,\dots,N_2-1\},\\
\bar\omega_h &= \{[ih_1, jh_2] \mid i = 0,\dots,N_1;\ j = 0,\dots,N_2\},\\
u_{ij} &= u(ih_1, jh_2),\\
u_{\bar x_1,ij} &= \frac{u_{ij}-u_{i-1,j}}{h_1},\ u_{x_1,ij} = \frac{u_{i+1,j}-u_{ij}}{h_1},\\
u_{\bar x_2,ij} &= \frac{u_{ij}-u_{i,j-1}}{h_2},\ u_{x_2,ij} = \frac{u_{i,j+1}-u_{ij}}{h_2},\\
\bar\nabla_h u &= [u_{\bar x_1}, u_{\bar x_2}],\quad \nabla_h u = [u_{x_1}, u_{x_2}].
\end{aligned}$$

We also use a projection operator $\mathcal{P}_h : \mathcal{C}(\Omega) \to \mathbb{R}^{N_1+1,N_2+1}$ defined as $\mathcal{P}_h g = g|_{\bar\omega_h}$. The discretization of the Neumann boundary conditions requires definition of the grid boundary normal difference $u_{\bar n}$:

$$
\begin{aligned}
&u_{\bar{n},0j} = u_{\bar{x}_1,1j} && \text{for } j = 0,\dots,N_2,\\
&u_{\bar{n},N_1 j} = u_{\bar{x}_1,N_1 j} && \text{for } j = 0,\dots,N_2,\\
&u_{\bar{n},i0} = u_{\bar{x}_2,i1} && \text{for } i = 0,\dots,N_1,\\
&u_{\bar{n},iN_2} = u_{\bar{x}_2,iN_2} && \text{for } i = 0,\dots,N_1.
\end{aligned}
$$

We define the following expressions:

$$
\begin{aligned}
(f,g)_h &= \sum_{i,j=1}^{N_1-1,N_2-1} h_1 h_2 f_{ij} g_{ij}, \quad \|f\|_h^2 = (f,f)_h\,,\\
(f^1, g^1\rfloor &= \sum_{i=1,j=1}^{N_1,N_2-1} h_1 h_2 f^1_{ij} g^1_{ij},\\
(f^2, g^2\rceil &= \sum_{i=1,j=1}^{N_1-1,N_2} h_1 h_2 f^2_{ij} g^2_{ij},\\
(\mathbf{f},\mathbf{g}] &= (f^1, g^1\rfloor + (f^2, g^2\rceil, \quad \|\mathbf{f}]|^2 = (\mathbf{f},\mathbf{f}],\\
(f,g] &= \sum_{i,j=1}^{N_1,N_2} h_1 h_2 f_{ij} g_{ij},
\end{aligned}
$$

where $\mathbf{f} = [f^1, f^2]$ and $\mathbf{g} = [g^1, g^2]$.

For the purpose of analysis, we recall the grid version of Green's formula proved in [5]:

LEMMA 4.1. *Let $p, u, v : \bar{\omega}_h \to \mathbb{R}$. Then Green's formula is valid:*

$$
\begin{aligned}
&(\nabla_h \cdot (p\bar{\nabla}_h u), v)_h = -(p\bar{\nabla}_h u, \bar{\nabla}_h v] \\
&+ \sum_{j=1}^{N_2-1} h_2 (p u_{\bar{x}_1}|_{N_1 j} v_{N_1 j} - p u_{\bar{x}_1}|_{1j} v_{0j}) + \sum_{i=1}^{N_1-1} h_1 (p u_{\bar{x}_2}|_{iN_2} v_{iN_2} - p u_{\bar{x}_2}|_{i1} v_{i0}).
\end{aligned} \tag{4.1}
$$

Then, we propose a semi-discrete scheme containing a time-dependent system of ODEs for the unknown functions $\Phi^h, H^h : (0,T) \times \bar{\omega}_h \to \mathbb{R}$

$$
\frac{d\Phi^h}{dt} = \nabla_h \cdot \left(Q(\bar{\nabla}_h \Phi^h)(\bar{\nabla}_h (H^h + F) - (\bar{\nabla}_h (H^h + F) \cdot \mathbf{N}^h)\mathbf{N}^h \right), \tag{4.2}
$$

$$
H^h = -\nabla_h \cdot \left(\frac{\bar{\nabla}_h \Phi}{Q(\bar{\nabla}_h \Phi^h)} \right), \quad \mathbf{N}^h = -\frac{\bar{\nabla}_h \Phi^h}{Q(\bar{\nabla}_h \Phi^h)}. \tag{4.3}
$$

According to (2.3)/(2.4), we consider two pairs of boundary conditions, alternatively:

$$
\Phi^h\big|_{\gamma_h} = 0, \quad H^h\big|_{\gamma_h} = 0, \tag{4.4}
$$

or

$$
\Phi^h_{\bar{n}}\big|_{\gamma_h} = 0, \quad H^h_{\bar{n}}\big|_{\gamma_h} = 0. \tag{4.5}
$$

The initial condition is written as follows

$$
\Phi^h\big|_{t=0} = \mathcal{P}_h \Phi_{ini}.
$$

The scheme (4.2) is a system of first-order differential equations in the initial-value problem. We resolve it by means of the Runge-Kutta method with the step adaptivity (Merson variant) as described in [15] and as used e.g. in [5], [4].

The scheme (4.2) satisfies the following features:

LEMMA 4.2. *Let Φ^h, H^h be a solution to the initial-boundary value problem (4.2) with $F = 0$. Then the following property holds*

$$\frac{d}{dt}(\Phi^h, 1)_h = 0,$$

provided the boundary conditions (4.5) are imposed.

Proof. We sum (4.2) over ω_h and use (4.1):

$$\frac{d}{dt}(\Phi^h, 1)_h = + \sum_{j=1}^{N_2-1} h_2(E_h^1|_{N_1 j} - E_h^1|_{1j}) + \sum_{i=1}^{N_1-1} h_1(E_h^2|_{iN_2} - E_h^2|_{i1}),$$

where we have denoted

$$\mathbf{E}_h = Q(\bar\nabla_h \Phi^h)(\bar\nabla_h(H^h + F) - (\bar\nabla_h(H^h + F)\cdot \mathbf{N}^h)\mathbf{N}^h, \quad \mathbf{E}_h = [E_h^1, E_h^2]. \tag{4.6}$$

The boundary conditions (4.5) and the assumption $F = 0$ imply that

$$(\Phi^h)_{\bar n}\big|_{\gamma_h} = 0, \quad (H^h + F)_{\bar n}\big|_{\gamma_h} = 0,$$

which yields the statement. **q.e.d.**

LEMMA 4.3. *Let $\bar\omega_h$ be a rectangular uniform mesh and let Φ^h, H^h be a solution to the semi-discrete initial value problem (4.2) with $F = 0$. Then the equality*

$$\frac{d}{dt}(Q(\bar\nabla_h\Phi^h), 1] + ((|\bar\nabla_h H^h|^2 - |\bar\nabla_h H^h \cdot \mathbf{N}^h|^2)\, Q(\bar\nabla_h\Phi^h), 1)_h = 0,$$

holds provided the boundary conditions (4.4) are imposed, and the equality

$$\frac{d}{dt}(Q(\bar\nabla_h\Phi^h), 1)_h + ((|\bar\nabla_h H^h|^2 - |\bar\nabla_h H^h \cdot \mathbf{N}^h|^2)\, Q(\bar\nabla_h\Phi^h), 1)_h = 0,$$

holds provided the boundary conditions (4.5) are imposed

Proof. We multiply the equation (4.2) by H^h and sum over ω_h:

$$(\frac{d\Phi^h}{dt}, H^h)_h = (\nabla_h \cdot \left(Q(\bar\nabla_h\Phi^h)(\bar\nabla_h(H^h + F) - (\bar\nabla_h(H^h + F)\cdot \mathbf{N}^h)\mathbf{N}^h\right), H^h)_h. \tag{4.7}$$

The left-hand side of (4.7) becomes

$$(\frac{d\Phi^h}{dt}, H^h)_h = -(\frac{d\Phi^h}{dt}, \nabla_h \cdot \frac{\bar\nabla_h\Phi^h}{Q(\bar\nabla_h\Phi^h)})_h = (\bar\nabla_h \frac{d\Phi^h}{dt}, \frac{1}{Q(\bar\nabla_h\Phi^h)}\bar\nabla_h\Phi^h]$$
$$- \sum_{j=1}^{N_2-1} h_2(\frac{1}{Q(\bar\nabla_h\Phi^h)}\Phi^h_{\bar x_1}|_{N_1 j}\ \frac{d\Phi^h}{dt}\Big|_{N_1 j} - \frac{1}{Q(\bar\nabla_h\Phi^h)}\Phi^h_{\bar x_1}|_{1j}\ \frac{d\Phi^h}{dt}\Big|_{0j})$$
$$- \sum_{i=1}^{N_1-1} h_1(\frac{1}{Q(\bar\nabla_h\Phi^h)}\Phi^h_{\bar x_2}|_{iN_2}\ \frac{d\Phi^h}{dt}\Big|_{iN_2} - \frac{1}{Q(\bar\nabla_h\Phi^h)}\Phi^h_{\bar x_2}|_{i1}\ \frac{d\Phi^h}{dt}\Big|_{i0}),$$

where the boundary expressions vanish due to (4.4)/(4.5). The expression

$$(\bar\nabla_h \frac{d\Phi^h}{dt}, \frac{1}{Q(\bar\nabla_h\Phi^h)}\bar\nabla_h\Phi^h] = \sum_{i=1}^{N_1}\sum_{j=1}^{N_2-1} h_1 h_2\ \frac{d\Phi^h}{dt}\Big|_{\bar x_1, ij}\ \frac{1}{Q(\bar\nabla_h\Phi^h)_{ij}}\Phi^h_{\bar x_1, ij}$$
$$+ \sum_{i=1}^{N_1-1}\sum_{j=1}^{N_2} h_1 h_2\ \frac{d\Phi^h}{dt}\Big|_{\bar x_2, ij}\ \frac{1}{Q(\bar\nabla_h\Phi^h)_{ij}}\Phi^h_{\bar x_2, ij}.$$

For the conditions (4.4), it becomes

$$\sum_{i=1}^{N_1}\sum_{j=1}^{N_2} h_1h_2\ \frac{d\Phi^h}{dt}\Big|_{\bar{x}_1,ij}\ \frac{1}{Q(\bar{\nabla}_h\Phi^h)_{ij}}\Phi^h_{\bar{x}_1,ij} + \sum_{i=1}^{N_1}\sum_{j=1}^{N_2} h_1h_2\ \frac{d\Phi^h}{dt}\Big|_{\bar{x}_2,ij}\ \frac{1}{Q(\bar{\nabla}_h\Phi^h)_{ij}}\Phi^h_{\bar{x}_2,ij}$$
$$= \frac{d}{dt}(Q(\bar{\nabla}_h\Phi^h),1],$$

and for the conditions (4.5), it becomes

$$\sum_{i=1}^{N_1-1}\sum_{j=1}^{N_2-1} h_1h_2\ \frac{d\Phi^h}{dt}\Big|_{\bar{x}_1,ij}\ \frac{1}{Q(\bar{\nabla}_h\Phi^h)_{ij}}\Phi^h_{\bar{x}_1,ij} + \sum_{i=1}^{N_1-1}\sum_{j=1}^{N_2-1} h_1h_2\ \frac{d\Phi^h}{dt}\Big|_{\bar{x}_2,ij}\ \frac{1}{Q(\bar{\nabla}_h\Phi^h)_{ij}}\Phi^h_{\bar{x}_2,ij}$$
$$= \frac{d}{dt}(Q(\bar{\nabla}_h\Phi^h),1)_h,$$

We then have

$$(\frac{d\Phi^h}{dt}, H^h)_h = \frac{d}{dt}(Q(\bar{\nabla}_h\Phi^h),1],$$

for the conditions (4.4), and

$$(\frac{d\Phi^h}{dt}, H^h)_h = \frac{d}{dt}(Q(\bar{\nabla}_h\Phi^h),1)_h,$$

for the conditions (4.5).

The right-hand side of (4.7) becomes

$$(\nabla_h\cdot\mathbf{E}_h, H^h)_h = -(\mathbf{E}_h, \bar{\nabla}_h H^h]$$
$$+\sum_{j=1}^{N_2-1} h_2(E^1_h|_{N_1 j}H^h|_{N_1 j} - E^1_h|_{1j}H^h|_{0j}) + \sum_{i=1}^{N_1-1} h_1(E^2_h|_{iN_2}H^h|_{iN_2} - E^2_h|_{i1}H^h|_{i0}),$$

where again the boundary expressions vanish due to (4.4)/(4.5). As $F=0$, we obtain

$$\frac{d}{dt}(Q(\bar{\nabla}_h\Phi^h),1] + (\mathbf{E}_h, \bar{\nabla}_h H^h] = 0,$$

in other words

$$\frac{d}{dt}(Q(\bar{\nabla}_h\Phi^h),1] + ((|\bar{\nabla}_h H^h|^2 - |\bar{\nabla}_h H^h\cdot\mathbf{N}^h|^2)\, Q(\bar{\nabla}_h\Phi^h),1)_h = 0,$$

for the conditions (4.4), and

$$\frac{d}{dt}(Q(\bar{\nabla}_h\Phi^h),1)_h + ((|\bar{\nabla}_h H^h|^2 - |\bar{\nabla}_h H^h\cdot\mathbf{N}^h|^2)\, Q(\bar{\nabla}_h\Phi^h),1)_h = 0,$$

for the conditions (4.5). **q.e.d.**

Remark. The boundedness of the expression $(Q(\bar{\nabla}_h\Phi^h),1)_h$, resp. $(Q(\bar{\nabla}_h\Phi^h),1]$ is obtained by means of the estimate

$$|\bar{\nabla}_h H^h|^2 - |\bar{\nabla}_h H^h\cdot\mathbf{N}^h|^2 \geq |\bar{\nabla}_h H^h|^2(1 - \frac{|\bar{\nabla}_h\Phi^h|^2}{Q(\bar{\nabla}_h\Phi^h)^2}) = \frac{|\bar{\nabla}_h H^h|^2}{Q(\bar{\nabla}_h\Phi^h)^2} \geq 0,$$

and by integration of the estimate for $(Q(\bar{\nabla}_h\Phi^h),1)_h$, resp. $(Q(\bar{\nabla}_h\Phi^h),1]$ over the time interval.

LEMMA 4.4. *Let $\bar{\omega}_h$ be a rectangular uniform mesh and let Φ^h, H^h be a solution to the semi-discrete initial value problem (4.2) with boundary conditions (4.4), or (4.5) with $F_{\bar{n}}|_{\gamma_h} = 0$. Then the following property holds*

$$\frac{1}{2}\frac{d}{dt}\|\Phi^h\|_h^2 + \|H^h\|_h^2 \leq \sqrt{L_1L_2}\|\bar{\nabla}_h F]|.$$

Proof. We again use the expression (4.6), multiply first equation in (4.2) by Φ^h, sum over ω_h and use (4.1):

$$\begin{aligned}&\frac{1}{2}\frac{d}{dt}\|\Phi^h\|_h^2 = -(E_h, \bar{\nabla}_h\Phi^h]\\ &+\sum_{j=1}^{N_2-1} h_2(E_h^1|_{N_1 j}\Phi^h|_{N_1 j} - E_h^1|_{1j}\Phi^h|_{0j}) + \sum_{i=1}^{N_1-1} h_1(E_h^2|_{iN_2}\Phi^h|_{iN_2} - E_h^2|_{i1}\Phi^h|_{i0}),\end{aligned}$$

where the boundary expressions vanish due to the conditions (4.4), or (4.5) with $F_{\bar{n}}|_{\gamma_h} = 0$. The remaining term becomes

$$\begin{aligned}(\mathbf{E}_h, \bar{\nabla}_h\Phi^h] &= (Q(\bar{\nabla}_h\Phi^h)(\bar{\nabla}_h H^h - (\bar{\nabla}_h H^h\cdot\mathbf{N}^h)\mathbf{N}^h), \bar{\nabla}_h\Phi^h]\\ &\quad +(Q(\bar{\nabla}_h\Phi^h)(\bar{\nabla}_h F - (\bar{\nabla}_h F\cdot\mathbf{N}^h)\mathbf{N}^h), \bar{\nabla}_h\Phi^h].\end{aligned}$$

We realize that for $g = H^h$, or $g = F$ we have

$$\begin{aligned}&\bar{\nabla}_h g\cdot\bar{\nabla}_h\Phi^h - (\bar{\nabla}_h g\cdot\mathbf{N}^h)(\mathbf{N}^h\cdot\bar{\nabla}_h\Phi^h)\\ &= \bar{\nabla}_h g\cdot\bar{\nabla}_h\Phi^h - \frac{1}{Q(\bar{\nabla}_h\Phi^h)^2}(\bar{\nabla}_h g\cdot\bar{\nabla}_h\Phi^h)|\bar{\nabla}_h\Phi^h|^2\\ &= \frac{1}{Q(\bar{\nabla}_h\Phi^h)^2}(\bar{\nabla}_h g\cdot\bar{\nabla}_h\Phi^h).\end{aligned}$$

We then obtain that

$$(\mathbf{E}_h, \bar{\nabla}_h\Phi^h] = (\frac{1}{Q(\bar{\nabla}_h\Phi^h)}\bar{\nabla}_h H^h, \bar{\nabla}_h\Phi^h] + (\frac{1}{Q(\bar{\nabla}_h\Phi^h)}\bar{\nabla}_h F, \bar{\nabla}_h\Phi^h].$$

Testing the definition of H^h (4.3) by H^h itself, Green's formula gives

$$\begin{aligned}(H^h, H^h)_h &= -(\nabla_h\cdot(\frac{\bar{\nabla}_h\Phi^h}{Q(\bar{\nabla}_h\Phi^h)}), H^h)_h\\ &= (\bar{\nabla}_h H^h, \frac{\bar{\nabla}_h\Phi^h}{Q(\bar{\nabla}_h\Phi^h)}]\\ &\quad -\sum_{j=1}^{N_2-1} h_2(\frac{1}{Q(\bar{\nabla}_h\Phi^h)}H^h|_{N_1 j}\Phi^h_{\bar{x}_1}|_{N_1 j} - \frac{1}{Q(\bar{\nabla}_h\Phi^h)}H^h|_{1j}\Phi^h_{\bar{x}_1}|_{0j})\\ &\quad -\sum_{i=1}^{N_1-1} h_1(\frac{1}{Q(\bar{\nabla}_h\Phi^h)}H^h|_{iN_2}\Phi^h_{\bar{x}_2}|_{iN_2} - \frac{1}{Q(\bar{\nabla}_h\Phi^h)}H^h|_{i1}\Phi^h_{\bar{x}_1}|_{i0}),\end{aligned}$$

where the boundary expressions vanish again due to (4.4), or (4.5). Finally, we obtain the energy equality

$$\frac{1}{2}\frac{d}{dt}\|\Phi^h\|_h^2 + (H^h, H^h)_h = (\frac{1}{Q(\bar{\nabla}_h\Phi^h)}\bar{\nabla}_h F, \bar{\nabla}_h\Phi^h],$$

leading by the fact that $\frac{|\bar{\nabla}_h\Phi^h|}{Q(\bar{\nabla}_h\Phi^h)} \leq 1$ to the desired result. **q.e.d.**

As a consequence, the solution Φ^h, H^h exists on a common time interval $(0, T)$.

5. Computational results. We have performed a series of computations by using (4.2) to show that it yields a good approximation of the original problem and to investigate the solution itself. First, we show the quantitative solution analysis for one-dimensional settings. Here, we measure the difference between two computations by means of the following norms:

$$\text{Error}_{\text{L}_\infty-\text{L}_2} = \max_{t\in\langle 0,T\rangle}\left(\int_\Omega |\mathcal{I}_h\Phi^h - \mathcal{I}_{\tilde{h}}\Phi^{\tilde{h}}|^2 dx\right)^{\frac{1}{2}},$$

$$\text{Error}_{\text{L}_\infty-\text{L}_\infty} = \max_{t\in\langle 0,T\rangle}\max_{x\in\Omega}|\mathcal{I}_h\Phi^h - \mathcal{I}_{\tilde{h}}\Phi^{\tilde{h}}|,$$

where $\mathcal{I}_h$ is the piece-wise linear interpolation operator. We evaluate the experimental order of convergence defined as follows

$$\frac{\text{Error}_h}{\text{Error}_{\tilde{h}}} = \left(\frac{h}{\tilde{h}}\right)^{EOC}.$$

In the computations, we use the boundary conditions (4.5) and the forcing term in the form stimulating the pinch-off as $F = \frac{C_F}{\Phi}$. The parameter Δt means the period of the data output, N_T number of such outputs, *tol* tolerance for the adaptive Mersn time stepping (see also [15]).

Example 1 evolves a 1D perturbation which vanishes after a time. We measure the difference between the particular numerical solution and the finest-grid solution. The problem setting and the finest-grid parameters are indicated in Table 5.3. The graph evolution is illustrated in Figure 5.1. The measured differences are summarized in Table 5.1 and the EOC's in Table 5.2. The CPU time is given by the system used in this case (LINUX RedHat 8.0 on the Pentium IV, 1.4 GHz, 756 MB RAM, the code compiled by the Intel Fortran Compiler 8.0).

Mesh h	N_T	$\text{Error}_{\text{L}_\infty-\text{L}_2}$	$\text{Error}_{\text{L}_\infty-\text{L}_\infty}$	CPU
0.0250000	10	0.0001783	0.0037160	0.4300000
0.0200000	10	0.0001145	0.0026200	1.3300000
0.0125000	10	0.0000467	0.0009820	13.3599997
0.0100000	10	0.0000350	0.0006600	40.8400002
0.0080000	10	0.0000248	0.0003950	124.8700027

TABLE 5.1
Table of numerical parameters and convergence errors for the Example 1.

Example 2 evolves a 1D perturbation which develops and increases in time ($C_F = -100.0$). We measure the difference between the particular numerical solution and the

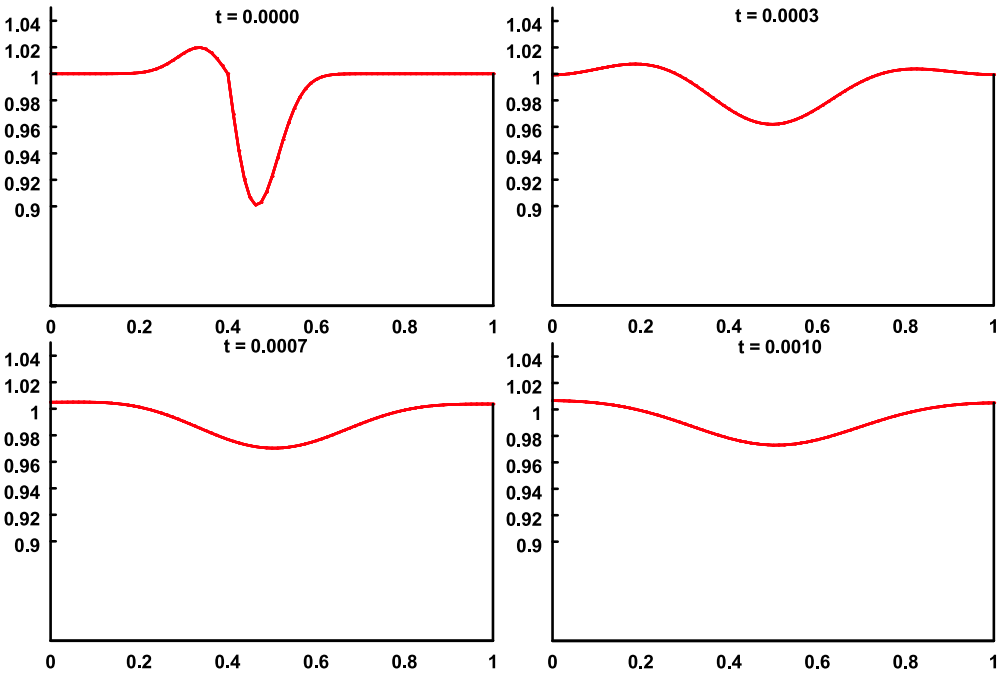

FIG. 5.1. *Example 1: The shape of the solution which tends to a constant value.*

Mesh h	N_T	EOC for $\text{Error}_{L_\infty - L_2}$	EOC for $\text{Error}_{L_\infty - L_\infty}$
0.0250000	10	0.0000000	0.0000000
0.0200000	10	1.9857855	1.5661373
0.0125000	10	1.9072390	2.0879377
0.0100000	10	1.2866584	1.7806986
0.0080000	10	1.5423961	2.3005560

TABLE 5.2
Table of EOC coefficients Error versus h for the Example 1.

finest-grid solution. The problem setting and the finest-grid parameters are indicated in Table 5.6. The graph evolution is illustrated in Figure 5.2. The measured differences are summarized in Table 5.4 and the EOC's in Table 5.5. The CPU time is given by the system used in this case (HP UX PARISC HP 8000 1 GHz processor, 12 GB RAM, the code compiled by the HP Fortran Compiler).

We proceed by the qualitative computational results indicating properties of the solution such as fast elimination of peaks and slow elimination of spatially larger variations of the initial condition.

Example 3 shows the situation when the initial perturbation simulating a surface crack develops and increases in time ($C_F = -100.0$). The problem setting and the numerical parameters are indicated in Table 5.7. The graph evolution is illustrated in Figure 5.3. The CPU time is given by the system used in this case (LINUX RedHat 8.0 on the Pentium IV, 1.4 GHz, 756 MB RAM, the code compiled by the Intel Fortran Compiler 8.0).

C_F	Ω	Δt	N_T	tol	mesh	CPU
0.0	(0,1)	0.00001	10	0.0001	0.005	1297.45

TABLE 5.3
Table of the finest experiment parameters for the Example 1.

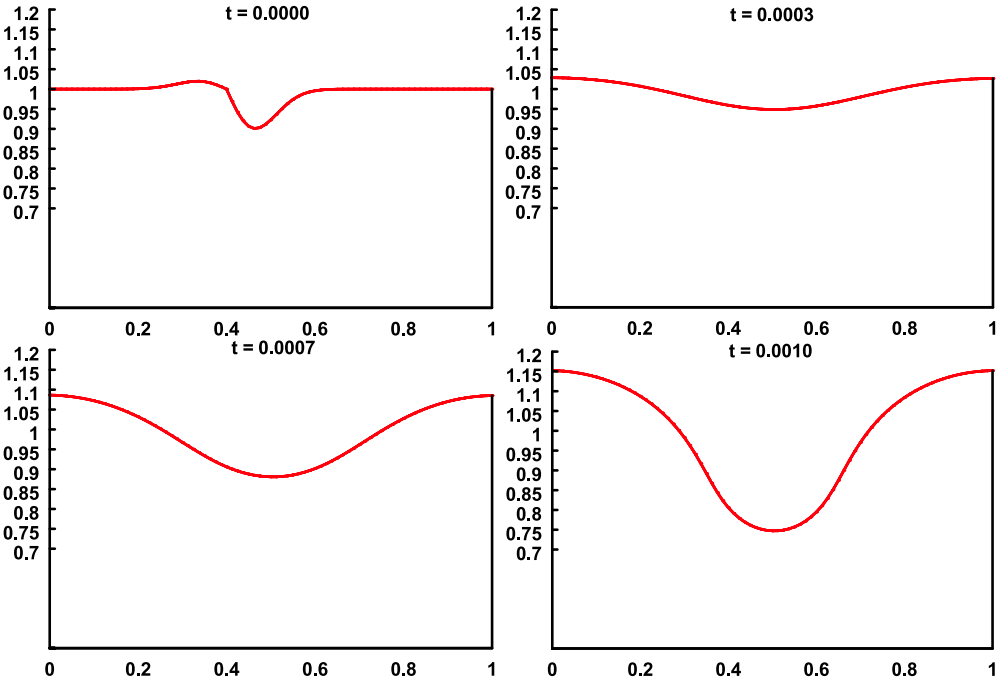

FIG. 5.2. *Example 2: The shape of the solution which develops in time.*

Mesh h	N_T	$\text{Error}_{L_\infty - L_2}$	$\text{Error}_{L_\infty - L_\infty}$	CPU
0.0250000	10	0.0031877	0.0214440	3.7200000
0.0200000	10	0.0023783	0.0160200	11.3599997
0.0125000	10	0.0009689	0.0061480	119.4100037
0.0100000	10	0.0004155	0.0021450	366.0799866

TABLE 5.4
Table of numerical parameters and convergence errors for the Example 2.

Mesh h	N_T	EOC for $\text{Error}_{L_\infty - L_2}$	EOC for $\text{Error}_{L_\infty - L_\infty}$
0.0250000	10	0.0000000	0.0000000
0.0200000	10	1.3127408	1.3068131
0.0125000	10	1.9104705	2.0376677
0.0100000	10	3.7947932	4.7188773

TABLE 5.5
Table of EOC coefficients Error versus h for the Example 2.

C_F	Ω	Δt	N_T	tol	mesh	CPU
-100.0	(0,1)	0.0001	10	0.0001	0.005	11833.26

TABLE 5.6
Table of the finest experiment parameters for the Example 2.

C_F	Ω	Δt	N_T	tol	mesh	CPU
-100.0	(0,1)x(0,0.5)	0.0001	11	0.0003	0.0166x0.0166	952.25

TABLE 5.7
Table of the experiment parameters for the Example 3.

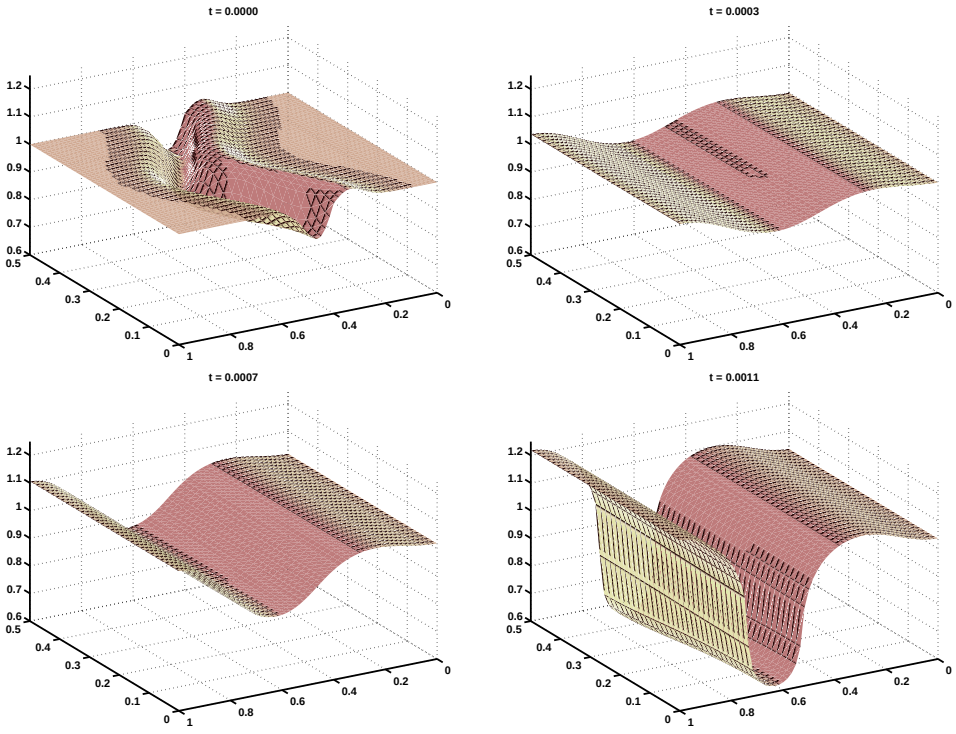

FIG. 5.3. *Example 3: The shape of the solution which develops in time.*

Example 4 shows the situation when the initial circular perturbation develops and increases in time ($C_F = -100.0$). The problem setting and the numerical parameters are indicated in Table 5.8. The graph evolution is illustrated in Figure 5.4. The CPU time is given by the system used in this case (LINUX RedHat 8.0 on the Pentium IV, 1.4 GHz, 756 MB RAM, the code compiled by the Intel Fortran Compiler 8.0).

C_F	Ω	Δt	N_T	tol	mesh	CPU
-100.0	(0,2)x(0,2)	0.00005	22	0.0003	0.02x0.02	2524.99

TABLE 5.8
Table of the experiment parameters for the Example 4.

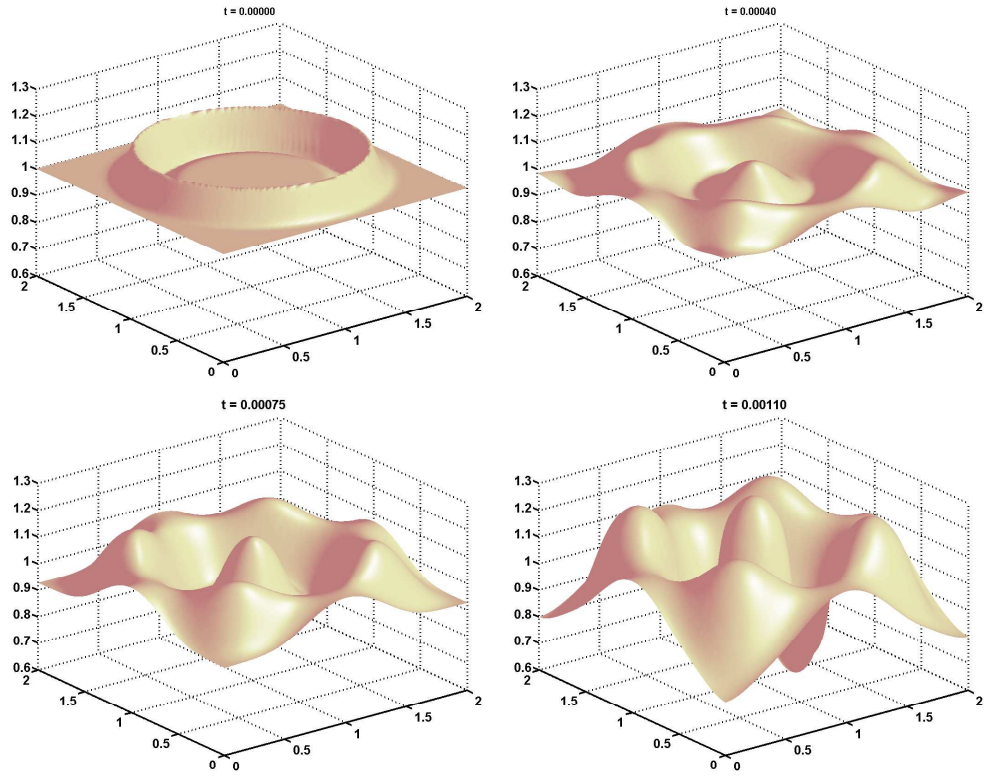

FIG. 5.4. *Example 4: The shape of the solution which develops in time.*

Example 5 shows the situation when the initial double-hill perturbation develops and is supressed in time. The problem setting and the numerical parameters are indicated in Table 5.9. The graph evolution is illustrated in Figure 5.5. The CPU time is given by the system used in this case (HP UX PARISC HP 8000 1 GHz processor, 12 GB RAM, the code compiled by the HP Fortran Compiler).

C_F	Ω	Δt	N_T	tol	mesh	CPU
0.0	(0,2)x(0,2)	0.0004	20	0.0003	0.02x0.02	8235.34

TABLE 5.9
Table of the experiment parameters for the Example 5.

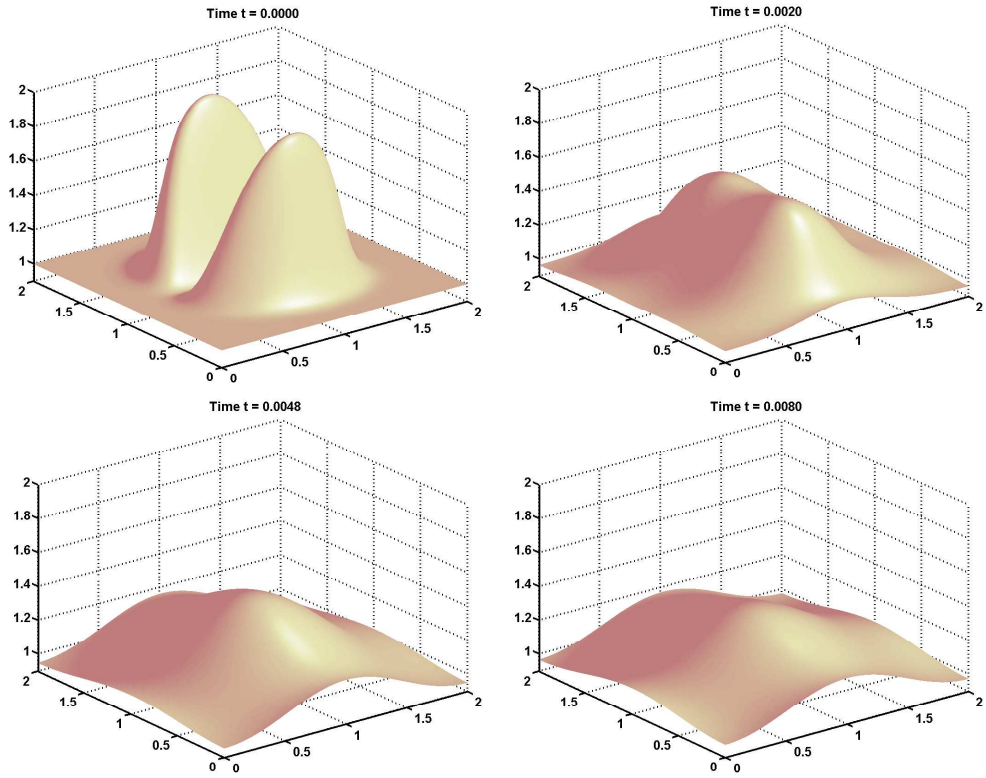

FIG. 5.5. *Example 5: The shape of the solution which develops in time.*

Example 6 shows the situation when the initial multi-hill perturbation develops and is supressed in time. The problem setting and the numerical parameters are indicated in Table 5.10. The graph evolution is illustrated in Figure 5.6. The CPU time is given by the system used in this case (HP UX PARISC HP 8000 1 GHz processor, 12 GB RAM, the code compiled by the HP Fortran Compiler).

6. Conclusion. In the article, we have presented the numerical scheme for the motion of graphs by surface Laplacian of the mean curvature based on the method of lines. The scheme has been analyzed concerning its stability features and used for the computation. We have demonstrated the numerical convergence as well as nonlinear behaviour of the solution leading to the crack formation.

C_F	Ω	Δt	N_T	tol	mesh	CPU
0.0	(0,2)x(0,2)	0.0003	60	0.0003	0.02x0.02	18682.61

TABLE 5.10
Table of the experiment parameters for the Example 6.

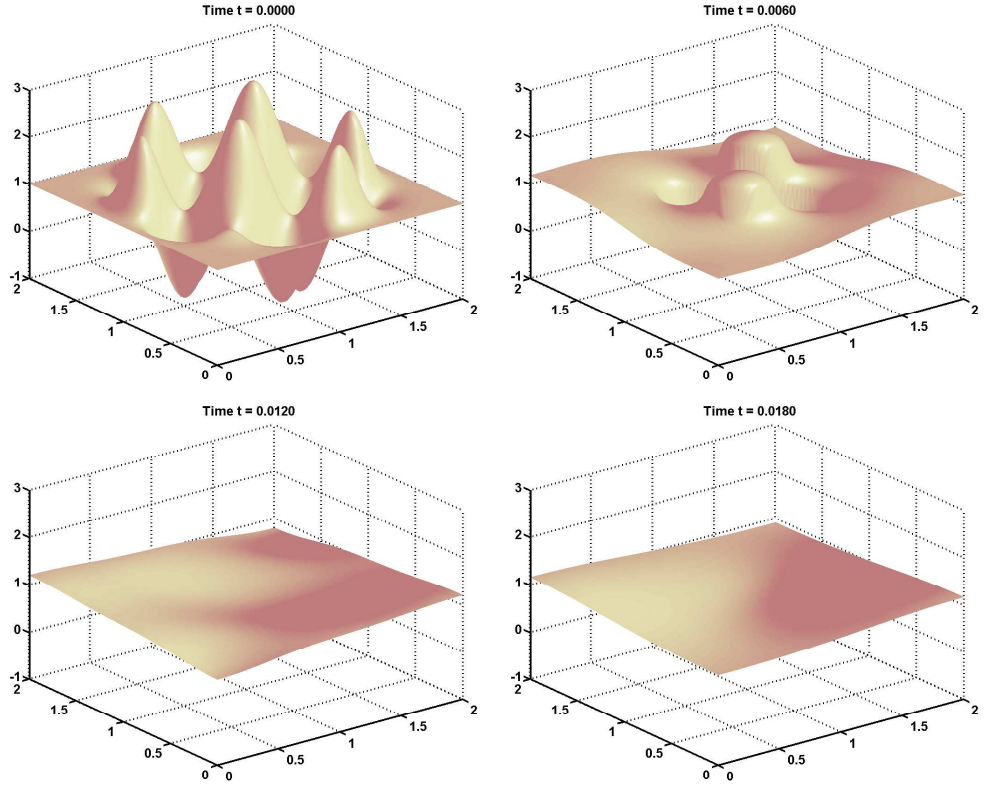

FIG. 5.6. *Example 6: The shape of the solution which develops in time.*

Acknowledgment. The author has been partly supported by the research branch of ČVUT No. MSM 6840770010 *"Applied Mathematics in Technical and Physical Sciences"*, and by the NSF grant NSF00-138 Award 0113555/Kontakt No. ME654 of the joint science programme between the Czech Republic and the USA. The participation in the Czech-Japanese Seminar in Applied Mathematics 2005 was possible due to the support of the 21st Century COE Program *"Development of Dynamic Mathematics with High Functionality"* of the Graduate School of Mathematics, the Kyushu University in Fukuoka, Japan. The author would like to thank G. Dziuk and R.F. Holub for the stimulating discussions.

REFERENCES

[1] R.J. Asaro and W.A. Tiller. Interface morphology development during stress corrosion cracking: Part I. Via surface diffusion. *Met. Trans.*, 3:1789–1796, 1972.
[2] E. Bänsch, P. Morin, and R.H. Nochetto. Finite element methods for surface diffusion. Technical Report 805/2003, WIAS Preprints, 2003.

[3] E. Bänsch, P. Morin, and R.H. Nochetto. Surface diffusion of graphs: Variational formulation, error analysis, and simulation. *SIAM J. Numer. Anal.*, 42 (2):773–799, 2004.

[4] M. Beneš. Diffuse-interface treatment of the anisotropic mean-curvature flow. *Applications of Mathematics*, 48, No. 6:437–453, 2003.

[5] M. Beneš and K. Mikula. Simulation of anisotropic motion by mean curvature–comparison of phase-field and sharp-interface approaches. *Acta Math. Univ. Comenianae*, 67, No. 1, 1998. 17–42.

[6] J. Cahn and J. Taylor. Surface motion by surface diffusion. *Acta Metall. Mater.*, 42:1045–1063, 1994.

[7] B.D. Coleman, R.S. Falk, and M. Moakher. Space-time finite element methods for surface diffusion with applications to the theory of the stability of cylinders. *SIAM J. Sci. Comput.*, 17(6):1434–1448, 1996.

[8] F. Davì and M.E. Gurtin. On the motion of a phase interface by surface diffusion. *Z. Angew. Math. Phys.*, 7:467–490, 1990.

[9] G. Dziuk, K. Deckelnick, and C.M. Elliott. Error analysis of a semidiscrete numerical scheme for diffusion in axially symmetric surfaces. *SIAM J. Numer. Anal.*, 41(6):2161–2179, 2003.

[10] G. Dziuk, E. Kuwert, and R. Schätzle. Evolution of elastic curves in $\mathbb{R}^n$: Existence and computation. *SIAM J. Math. Anal.*, 33(5):1228–1245, 2002.

[11] C.M. Elliott and S. Maier-Paape. Loosing graph with surface diffusion. *Hokkaido Math. J.*, 30:297–305, 2001.

[12] J. Escher, U.F. Mayer, and G. Simonett. The surface diffusion flow for immersed hypersurfaces. *SIAM J. Math. Anal.*, 29(6):1419–1433, 1998.

[13] N.M. Ghoniem. *Proceedings of the Second International Conference on Multiscale Materials Modeling*. UCLA Publication, Los Angeles, 2004.

[14] X. Han and N.M. Ghoniem. Stress field and interaction forces of dislocations in anisotropic multilayer thin films. *Phil. Mag.*, 85(11):1205–1225, 2005.

[15] M. Holodniok, A. Klíč, M. Kubíček, and M. Marek. *Methods of Analysis of Nonlinear Dynamical Models*. Academia, Prague, 1984.

[16] R.F. Holub, M. Beneš, and B.D. Honeyman. Interfacial phenomena in fluid dynamics: Linking atomistic and macroscopic properties: Can they explain the transport anomalies? In *Proceedings of Czech-Japanese Seminar in Applied Mathematics 2004, editors M. Beneš, J. Mikyška, T. Oberhuber*, pages 57–62, Prague, 2005. ISBN 80-01-03181-0.

[17] W.W. Mullins. Theory of thermal grooving. *J. Appl. Phys.*, 28(3):333–339, 1957.

[18] W.W. Mullins. The effect of thermal grooving on grain boundary motion. *Acta Metall.*, 6:414–427, 1958.

[19] T. Oberhuber. Numerical solution of the Willmore flow on graphs. submitted to the Proceedings on the Czech-Japanese Seminar in Applied Mathematics 2005, 2005.